Journal of Alloys and Compounds 513 (2012) 61–67

Contents lists available at SciVerse ScienceDirect

Journal of Alloys and Compounds

journal homepage: www.elsevier.com/locate/jallcom

Damping behavior in $Al_{18}B_4O_{33}w$/Al composite containing an interfacial layer with low melting point metal particles

J. Hu*, G. Liu, S.W. Tang

School of Materials Science and Engineering, Harbin Institute of Technology, Box 433, Harbin 150001, PR China

ARTICLE INFO

Article history:
Received 11 April 2011
Received in revised form 25 August 2011
Accepted 19 September 2011
Available online 13 October 2011

Keywords:
Metal matrix composites
Interface
Damping capacities
Microstructures

ABSTRACT

A $SnO_2{\cdot}Bi_2O_3$ coating was deposited on the surface of $Al_{18}B_4O_{33}$ whiskers. A pure aluminum matrix composite reinforced by an $Al_{18}B_4O_{33}$ whisker with $SnO_2{\cdot}Bi_2O_3$ coatings was fabricated by squeeze casting method. Sn and Bi particles were introduced to whisker/Al interface during the squeeze casting, resulting in the formation of the Bi–Sn two-component eutectic. The effects of the coating contents on the damping properties of the coated composites at various temperatures, frequencies, and strain amplitudes were examined. The results of the damping characterization indicated that the damping capacity of the coated composites strongly depends on the coating contents, strain amplitudes and vibration frequencies. A damping peak at about 150 °C appeared in the coated composites, and the damping mechanism is related to the interfacial slip caused by the molten Bi–Sn eutectic. A critical temperature in the damping-temperature curves of the coated composites has been found for the first time when the vibration frequencies changed. The dominant damping mechanisms changed from the dislocation damping to the interfacial damping below and above the critical temperature, respectively. The critical temperature decreases with the increasing of coating contents.

1. Introduction

Damping in metal matrix composites (MMCs) significantly affects their dynamic structure by controlling noise and vibration, and thus will prolong the service life of MMCs under the repeated loading or impact [1]. Therefore, a great deal of research has focused on the damping capacity of MMCs [2–4]. The performance of the composite depends on the matrix microstructure, the nature of the ceramic reinforcement and the matrix/reinforcement interface [5,6]. The effects of reinforcements, matrix alloys and reinforcement coatings on the damping capacity of MMCs have been studied widely [7–10].

The nature of the matrix/reinforcement interface within a composite often has a profound effect on its overall properties. The proper selection or design of interfacial phases plays a vital role in optimizing the final properties of MMCs [1,11]. The modification of the matrix composition and the chemical composition of the reinforcement has previously been employed to obtain desired interfaces with better properties [4,12,13]. Coatings of reinforcement by chemical vapour deposition (CVD), electroless, or sol–gel processes are some of the successfully adopted techniques [10,14,15].

As a new material, alumina borate whisker-reinforced aluminum composite ($Al_{18}B_4O_{33}w$/Al) has been considered for a wide range of applications [16].

Our previous study found that the presence of Sn or Bi particles at the $Al_{18}B_4O_{33}w$/Al interface plays a very important role in the damping properties of the composites reinforced with the SnO_2-coated and Bi_2O_3-coated whisker [17,18]. Two damping peaks were observed in both coated composites. The damping peak at lower temperatures (for temperatures lower than 200 °C) was related to the dislocation motion and interfacial slip at the whisker/Sn(Bi) because the damping capacities of the peak depended not only on the strain amplitudes but also on their coating contents. The damping peak at higher temperatures (for temperatures higher than 200 °C) was attributed to the Sn (or Bi) melting which occurred with interface slip at the whisker/Al.

In Ref. [19], a SnO_2–Bi_2O_3 layer was deposited on the surface of the $Al_{18}B_4O_{33}$ whisker (ABOw). Pure Sn and Bi particles have been introduced at the interface in the ABOw-reinforced pure aluminum matrix composite. Only one damping peak was found on the damping capacity-temperature curves of the $SnO_2{\cdot}Bi_2O_3$-coated ABOw/Al composites when the whisker preform was sintered at 500 °C. However, the damping mechanism of the peak is still not completely clear.

In this work, the effects of coating contents on the damping capacities of the coated ABOw/Al composites at various strain amplitudes and vibration frequencies were examined and the damping mechanisms of the coated composites were also

* Corresponding author. Tel.: +86 451 86415894; fax: +86 451 86413922.
E-mail address: hujin@hit.edu.cn (J. Hu).

0925-8388/$ – see front matter © 2011 Elsevier B.V. All rights reserved.
doi:10.1016/j.jallcom.2011.09.073

Table 1
Specification for the ABOw/Al composites with different $SnO_2{\cdot}Bi_2O_3$ coating contents.

Mass radio between whisker and coating	Coating contents in composites (mass%)	Composites
20:1	1.06	20ABOw/SnBiO/Al
10:1	2.10	10ABOw/SnBiO/Al
6:1	3.45	6ABOw/SnBiO/Al

discussed. Its results will be very useful for the understanding of the damping mechanism for MMCs.

2. Experiments

A $SnO_2{\cdot}Bi_2O_3$ layer was deposited on the surface of the ABOw with a diameter of 0.5–1.5 μm and length of 10–30 μm using a chemical method.

Firstly, a mixed nitrate solution involving Sn and Bi (the molar ratio of Sn salt and Bi salt is 4:3, near the eutectic composition) was put into HNO_3 solution (pH 1), avoiding the interaction between Sn salt and Bi salt solution. Subsequently, whiskers were put into the mixed solution. The mass ratio between ABOw and $SnO_2 + Bi_2O_3$ was set as 10:1. Secondly, NH_4OH water solution was dribbled into the mixed solution with the whiskers. With the addition of NH_4OH, $Sn(OH)_4$ and $Bi(OH)_3$ began to deposit on the whisker surfaces. Finally, putting the whisker with hydroxide coatings into a mould, and filtrating and pressing the coated whisker, a whisker preform could be formed.

The whisker preform was sintered at 500 °C for 1 h to avoid the reaction between SnO_2 and Bi_2O_3 occurring (our previous study found that SnO_2 can react with Bi_2O_3 when the temperature exceeds 605 °C and the reaction product was $Bi_2Sn_2O_7$ [19]). The whisker preform was put into a mould, preheated at 480–520 °C, and then pure Al at 780–800 °C was cast into the mould with a pressure of 80–100 MPa, which was held for 10 min. The ABOw/Al composite was fabricated by the squeeze casting technique. SnO_2 and Bi_2O_3 can react with molten Al during the squeeze casting process. Pure Sn and Bi particles were introduced together at the interface in the ABOw/Al composite, which could be accompanied with a mixing reaction of Sn and Bi atoms resulting in the formation of the Bi–Sn eutectic.

The volume fraction of the ABO whiskers was about 20%. The mass ratios between the ABOw and the coatings were set as 6:1, 10:1, and 20:1, respectively. The corresponding abbreviations are listed in Table 1.

The phase compositions of the coated whiskers and the coated composites were identified using a Philips X'Pert x-ray diffractometer (XRD) with Cu Kα radiation. The morphologies of coated whiskers were examined by a Hitch S-4700N scanning electron microscope (SEM). The microstructures of the coated composites were investigated using a Philips CM-12 transmission electron microscopy (TEM). High-angle annular dark field (HAADF) and high-resolution TEM (HRTEM) were carried out to understand the interfacial structure in the most direct and accurate way.

The damping capacities of the studied composites were investigated by a dynamic mechanical analyzer with a single cantilever vibration mode. At least three samples for each material were tested to verify repeatability. The gauge dimension of the damping specimen was 38 mm × 4 mm × 1 mm. The damping capacity was determined by $Q^{-1} = \tan\delta$ [20], where δ was the lag angle between the applied strain and response stress. Temperature dependent damping tests were made at various strains (ε) from 4×10^{-5} to 8×10^{-4} and various vibration frequencies (f) from 0.5 to 70 Hz, and the temperature (T) range was from 25 to 400 °C.

3. Results

3.1. Characterization of coated whiskers

The microstructure of the coated whiskers (after sintering) was investigated (Fig. 1). Fig. 1(a) shows XRD patterns of the coated whiskers. A broad diffraction peak (between 25° and 35°) appears in the coated whiskers, which displayed that amorphous phases were formed on the surface of whiskers. The broad peak should belong to Bi_2O_3 and SnO_2, they are the decomposition products of precursors $Bi(OH)_3$ and $Sn(OH)_4$ [19]. The morphologies of ABOw with and without the $SnO_2{\cdot}Bi_2O_3$ coatings were also observed. Fig. 1(b) shows the surface characteristics of ABOw, the surfaces of whiskers are smooth. Fig. 1(c) presents the backscattering electronic (BSE) image of the coated whiskers. It can be found that some bright zones presented at the whisker surfaces, and the bright zone is the SnO_2–Bi_2O_3 coatings (the Sn and/or Bi-rich phases) due to larger atomic numbers of the elements Sn and Bi. In addition, it can be observed that mixed coatings were non-continuously distributed on the surface of whiskers.

3.2. Microstructures of coated composites

Fig. 2(a) is the XRD patterns of the ABOw/SnBiO/Al composites. The XRD results revealed that pure Sn and Bi existed in the coated composites. It could be noticed that the intensities of the Sn and Bi peaks increased with the increase in coating contents, indicating more Sn and Bi could be introduced into the coated composites with increasing coating contents. Fig. 2(b) shows the HAADF image of the interfacial layer between Al and ABOw in the 10ABOw/SnBiO/Al composite. The energy dispersive X-ray spectroscopy (EDS) of the layer (a red cross in Fig. 2(b)) indicates that the mass ratio of Bi and Sn is 58:42, near the eutectic composition (Fig. 2(c)).

Based on the TEM and XRD analyses, it can be concluded that the $SnO_2{\cdot}Bi_2O_3$ layer reacted with molten aluminum during the squeeze casting process and that Sn and Bi could be formed. Moreover, Sn and Bi atoms could react to result in the formation of the Bi–Sn two-component eutectic, which melts at 139 °C [21]. The Bi–Sn eutectic was distributed at the whisker/matrix interfacial layer. The reaction equations may be as follows:

$$Bi_2O_3 + 2Al \rightarrow Al_2O_3 + 2Bi \quad (1)$$

$$3SnO_2 + 4Al \rightarrow 2Al_2O_3 + 3Sn \quad (2)$$

$$Bi + Sn \rightarrow Bi\text{–}Sn(\text{eutectic}) \quad (3)$$

Our previous study indicated that there are plenty of dislocation tangles in the matrix close to the interface of the ABOw/Al composite [25]. Fig. 3 shows TEM images of the 6ABOw/SnBiO/Al composite. The density of dislocations of the Al matrix adjacent to the interface of the composite is obviously low in the interfacial region with the interfacial layer (as shown in Fig. 3(a)). Fig. 3(b) and (c) shows that many dislocations exist in a Bi or Sn particle; these may be induced by the deformation under stress concentration.

As we know, the coefficients of thermal expansion (CTEs) are different between the whisker and aluminum matrix. As the ABOw/Al composite cooled from high temperatures, the great difference of CTEs would result in a high density of dislocations at the interface between the whisker and Al matrix [22]. Considering the Bi–Sn eutectic has a lower solidification temperature, the introduction of the Bi–Sn eutectic at the interface in the coated composites would reduce the mismatch strain when the composites are cooled from the elevated temperature of processing, and the corresponding dislocation may lessen.

The presence of the Bi–Sn eutectic at the interface in the coated composites changes not only the interface structure but also the density of the dislocations of the matrix in the vicinity of the interface, which will play an important role on the damping properties of the coated composites.

3.3. Damping properties of coated composites

3.3.1. Damping capacity of the coated composites at low frequencies

The curves of damping capacity versus temperature plotted for the ABOw/SnBiO/Al composites at lower frequencies (below 20 Hz) are shown in Fig. 4. The similar damping behavior could be observed in the three coated composites. The damping capacities of the coated composites increase with the increasing temperature and decreasing frequency and this increase is higher at lower frequencies.

From Fig. 4, it can be found that for every frequency; one visible damping peak appears in the coated composites. The height of the peak rapidly increased with the decreasing frequency. In

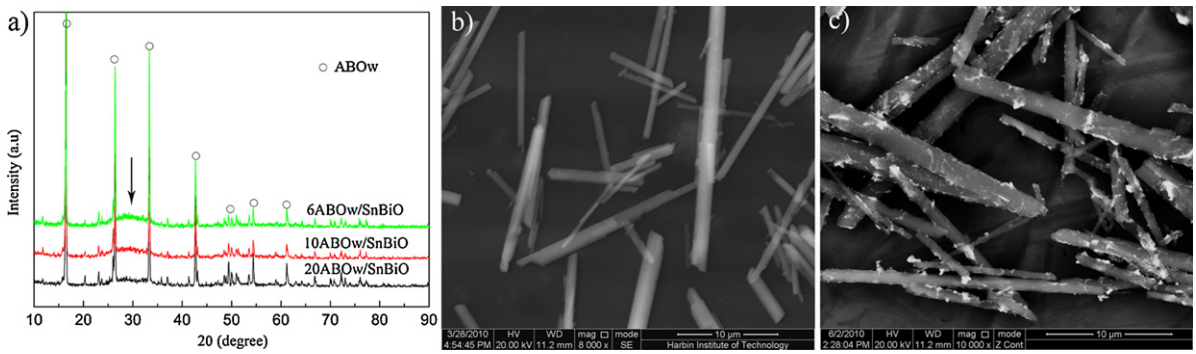

Fig. 1. Structure and morphology of the coated ABOw: (a) XRD patterns; (b) morphology of the uncoated whiskers; (c) morphology of the coated whiskers.

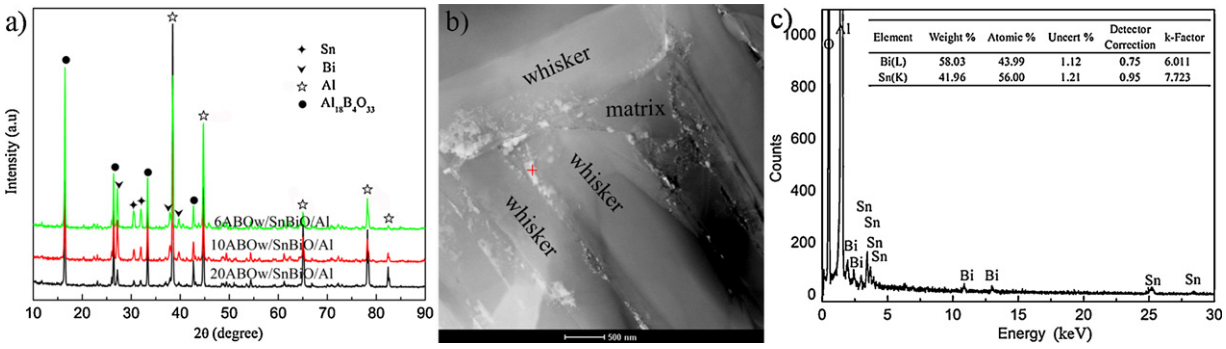

Fig. 2. Microstructure of the coated composites: (a) XRD patterns of the ABOw/SnBiO/Al composites; (b) HAADF image of the 10ABOw/SnBiO/Al composite; (c) the EDS of the interfacial layer in (b).

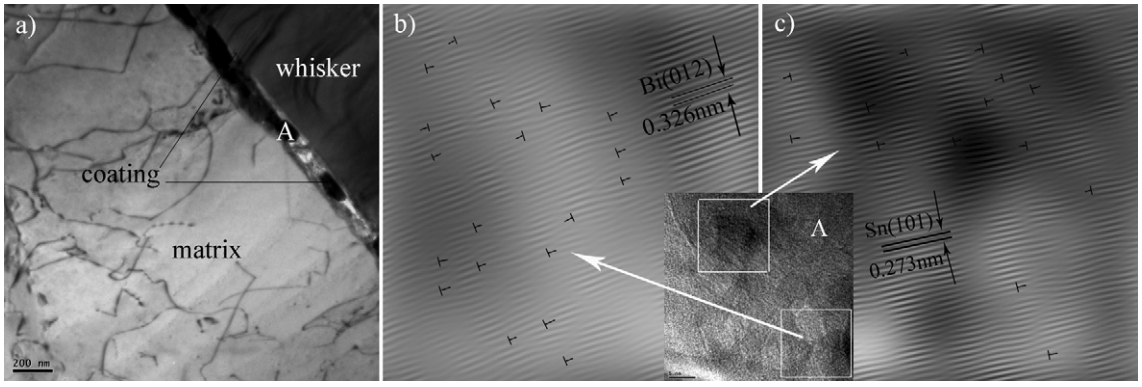

Fig. 3. TEM images of the 6ABOw/SnBiO/Al composite: (a) density of dislocations in the Al matrixes of the composite; (b) HRTEM image showing dislocation in a Bi particle; (c) HRTEM image showing dislocation in a Sn particle.

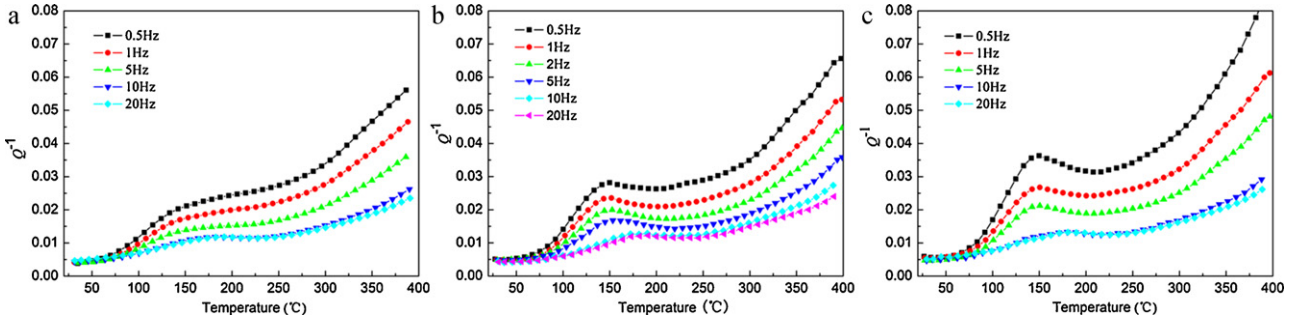

Fig. 4. Damping capacities of the ABOw/SnBiO/Al composites at lower frequencies (*f* below 20 Hz): (a) 20ABOw/SnBiO/Al; (b) 10ABOw/SnBiO/Al; (c) 6ABOw/SnBiO/Al.

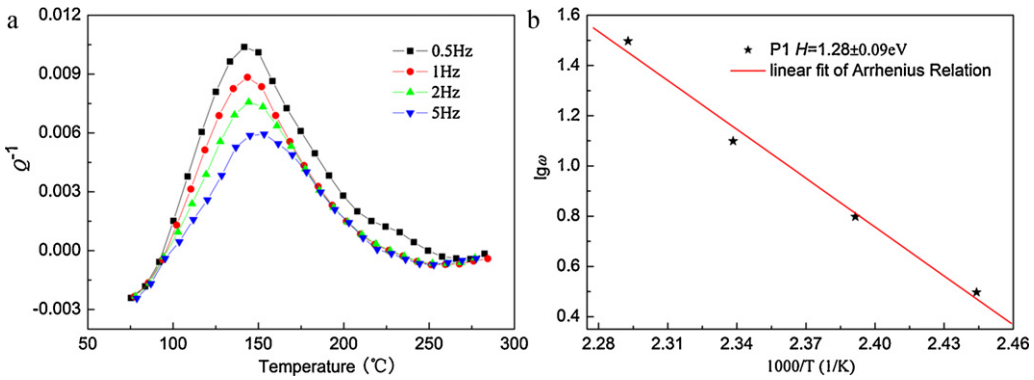

Fig. 5. (a) The damping peaks of the 10ABOw/SnBiO/Al composite at the different frequencies; (b) Arrhenius plot for peak observed in the 10ABOw/SnBiO/Al composite.

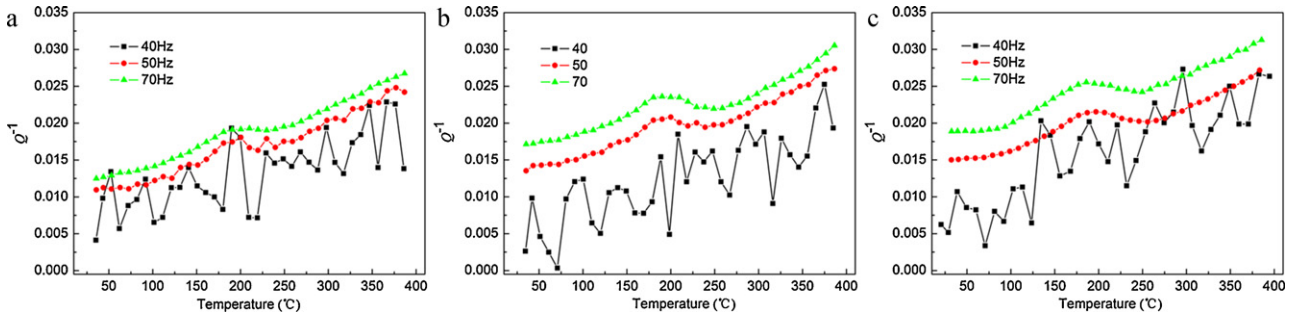

Fig. 6. Damping capacities of the ABOw/SnBiO/Al composites at higher frequencies (f beyond 40 Hz): (a) 20ABOw/SnBiO/Al; (b) 10ABOw/SnBiO/Al; (c) 6ABOw/SnBiO/Al.

addition, the peak became much clear with the increase in coating contents, which represented that the damping behavior of the coated composites strongly depended on the coating contents. Besides, some deflections from pure exponential curve after main damping peak are visible at temperatures corresponded to the melting points of Sn (232 °C) and Bi (271 °C). This fact allows expecting some inhomogenities in distribution of Bi and Sn atoms within interfacial layer. When the temperatures exceeded 270 °C, the damping capacities of the composite obviously depended on the temperature.

After subtracting the background damping consisted in an exponential term, the bare damping peaks at different frequencies were obtained. The enlarged damping peaks of the 10ABOw/SnBiO/Al composite are shown in Fig. 5(a). The damping peak in the coated composite shows a slight shift towards higher temperatures with increasing frequency. Table 2 lists the peak temperatures in the ABOw/SnBiO/Al composites. The activation parameters of the peak were determined using the Arrhenius equation. The Arrhenius plot of the 10ABOw/SnBiO/Al was obtained based on the data in Table 2, as shown in Fig. 5(b). Then the activation energies H for the peaks in the coated composites were calculated to be 1.36, 1.28 and 1.24 eV, respectively. The activation energy of the peak reduces as the coating content increases, which indicated that internal friction could easily appear in the coated composite with the higher coating contents.

Table 2
Variation of damping peak temperatures at various frequencies for the coated composites.

f (Hz)	20ABO/SnBiO/Al P1	10ABO/SnBiO/Al P1	6ABO/SnBiO/Al P1
0.5	143.5	136.0	133.7
1	152.5	145.1	142.5
2	–	154.3	–
5	170.6	162.5	162.2

3.3.2. *Damping capacities of the coated composite at high frequencies*

The effects of higher frequencies (above 40 Hz) on the damping capacities as a function of test temperatures for the ABOw/SnBiO/Al composites are shown in Fig. 6. A similar phenomenon could be found in the temperature-damping curves of the three coated composites. The damping capacities of the coated composites increased with temperature gradually and one damping peak at about 185 °C could still be seen in the coated composites. In addition, it can be found that the damping values of the coated composites increased with the increasing frequency dramatically. It is worth noting that an obvious undulation appeared at the damping-temperature curves of the coated composites when the frequency was 40 Hz. Moreover, a slight fluctuation of the damping values could also be seen at the damping-temperature curves when the frequency was 50 Hz. These phenomena indicated that the damping mechanisms of the coated composites had changed when the frequency changed. The 40 Hz may be a critical value for the change of the damping mechanism of the coated composites.

3.3.3. *Damping capacities of the coated composites at various strain amplitudes*

The effects of strain amplitude on the damping capacity (f = 0.5 Hz) as a function of test temperatures for the 10ABOw/SnBiO/Al composite are shown in Fig. 7. The damping capacity of the coated composite increased slightly with the increasing strain amplitude when the temperature was below 120 °C. A remarkable increase in the damping capacity took place above 120 °C, which indicated that more vibration energy was dissipated under higher strain amplitudes.

From Fig. 7, it can be observed that the height of the damping peak increased with the increase in strain amplitude. It is worth to note that the temperature of the damping peak almost had no change when strain amplitude increases. Therefore, one can

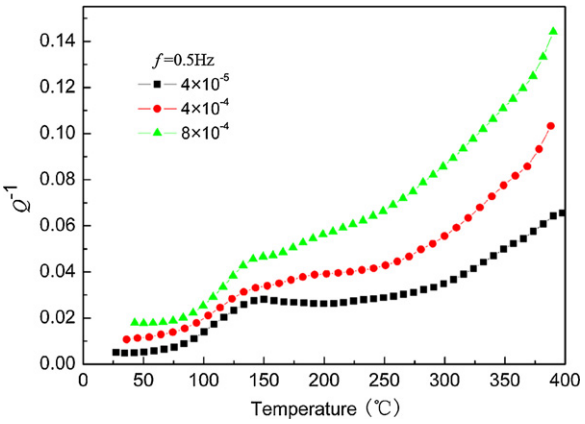

Fig. 7. Damping capacity of the 10ABOw/SnBiO/Al composite at various strain amplitudes (f = 0.5 Hz).

conclude that the damping mechanism of the coated composite does not change under different strain amplitudes.

Corresponding damping-temperature curves (f = 0.5 Hz) of the 20ABOw/SnBiO/Al and 6ABOw/SnBiO/Al composites at various strain amplitudes were also obtained. It was observed that the effects of temperature and strain amplitude on the damping capacities of the two coated composites are similar to that of the 10ABOw/SnBiO/Al composite.

3.3.4. Effect of coating contents on the damping capacities of the coated composites

Fig. 8 displays the effect of coating contents on the damping capacity of the coated composites. It can be observed that the damping capacities increased with the temperature for all the studied composites. Only one damping peak appeared in the all coated composites, the damping values increased with the increasing of coating contents, but the changes of peak temperatures were not obvious. Some deflections from pure exponential curve after main damping peak visible at temperatures corresponded to the melting points of Sn (232 °C) and Bi (271 °C) indicates to some inhomogenity in distribution of Bi and Sn atoms within interfacial layer. This inhomogenity almost vanishes when the coating content increases.

4. Discussions

4.1. Interfacial damping

In MMCs, dislocation damping of the matrix, reinforcement/matrix interface damping are the possible dominant damping mechanisms.

Several studies indicated that the matrices in MMCs contain high dislocation densities near the reinforcement/matrix interface [22,23]. The generation of high dislocation densities during the solidification of the ABOw/Al composite, resulting in a possible source of high damping presenting in the composite. A damping peak at about 150 °C was observed in the ABOw/Al composite [24]. A similar phenomenon was also found by Hu et al. [25]. They deduced that high dislocation densities at the interface of the whisker/Al, were generated due to thermal mismatch strain caused by the coefficients of thermal expansion between the whisker and the aluminum matrix, is the major source of damping.

Further studies [17,18] have found that a damping peak at about 134 °C and 94 °C appeared in the ABOw/Al composites with SnO_2 and Bi_2O_3 coatings, respectively, and the activation energies of the peaks were calculated to be 1.89 and 0.82, respectively. The damping mechanisms of the peak in both coated composites are attributed to the dislocation motion and the interfacial slip between the whisker/Sn(or Bi) because the damping capacities of the peak depend not only on the strain amplitudes but also on their coating contents. In addition, the dislocation damping peak shifted towards low temperatures with the increasing strain amplitude.

As we know, not only the temperatures but also the applied stress would increase the mobility of dislocations; therefore, the dislocation in the matrices of the coated composites will move at lower temperatures with the increase in applied stress. As a result of the motion, the density of moving dislocation increases with the increasing strain amplitudes. In this case, the damping peak should shift to lower temperatures as the strain amplitude increased.

Though, the damping capacity of the damping peak in this present study depends not only on the strain amplitudes but also on the coating contents. However, it is worthwhile to note that there were no peak shifts to be observed as the strain amplitudes increased. According to the above analysis, we considered that dislocation damping has a few contributions to improving the damping capacity of ABOw/SnBiO/Al composites. This may be attributed to the existence of the Bi–Sn eutectic in the interfacial layer, resulting in a low density of dislocations being present in the Al matrix close to the interface (Fig. 3(a)).

It is evident that the content of the Bi–Sn eutectic is proportional to that of the $SnO_2{\cdot}Bi_2O_3$, so the content of the Bi–Sn eutectic in the coated composites increases with increasing coating contents. The damping capacities of the coated composites increased with increasing coating contents, indicating that the damping properties of the coated composites are attributed to the presence of the Bi–Sn eutectic. It is strongly suggested that the damping mechanism of the peak in the ABOw/SnBiO/Al composite is attributed to the molten Bi–Sn eutectic (melting point is of 139 °C) which went with the interface slip at the whisker/interlayer and interlayer/Al interface. As the coating contents increased, more Bi–Sn eutectic formed in the coated composites, resulting in more interface movement. Thus, the damping capacities of the coated composites increased with the increasing of coating contents. In our previous studies [18,25], we also observed two damping peaks related to the interfacial sliding of molten Bi (at 271 °C) or Sn (at 232 °C). The temperature of the damping peak in the ABOw/SnBiO/Al composites is lower than that of in the SnO_2-coated and Bi_2O_3-coated composites [18,25] due to the low melting point of the Bi–Sn eutectic. Moreover, the damping values continuously increased with increasing temperature, which indicated that the interfacial slip at the whisker/Al interface and grain-boundary sliding all contributed to the damping.

The ABOw/SnBiO/Al composites show one damping peak, and the damping value keeps an almost constant range of 140–240 °C. The damping peak corresponds to the whisker/interlayer interfacial movement, Bi–Sn eutectic melting and whisker/Al interfacial movement. When the temperature is elevated, the interfacial layer becomes soft. Whereas there exists a weak interface between whisker and interfacial layer, a movement at the ABOw/interlayer is likely to occur when the magnitude of the shear stress at the interface is sufficient to overcome friction loads [3]. With the increasing of temperature, the energy dissipation resulted from the interfacial slip at the whisker/interlayer, the Bi–Sn eutectic melting and the interface slip at the whisker/Al interface will contribute to the damping capacities of the coated composites one by one, resulting in a similar platform appearing in the damping curves of the coated composites. Subsequently, the damping capacity has an increasing trend with increasing temperature. This is due, as many researchers have reported, to the interfacial damping (ABOw-Al) [24,25]. The presence of the liquid phase at the interface not only will provide melting damping but also will help the interface slip between reinforcement and matrix, thus the damping capacities of the coated composites continuously increased with the temperature (Fig. 8),

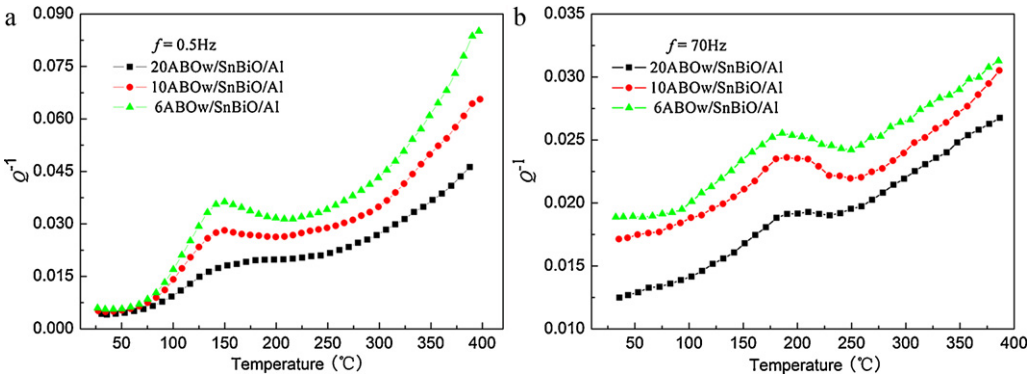

Fig. 8. Damping capacity of the ABOw/SnBiO/Al composites at different frequencies: (a) $f = 0.5$ Hz; (b) $f = 70$ Hz.

because of the melting, the Bi–Sn eutectic provided a high damping background for the coated composites.

4.2. Thermoelastic damping

From Fig. 5, it can be found that the damping peak in the 10ABOw/SnBiO/Al composite shifts to higher temperatures with the increase in frequencies, exhibiting the characteristics of a relaxation type.

According to Zener's thermoelastic theory [26], thermoelastic damping increases with increasing frequencies when testing frequency below Zener relaxation frequency [27]. In this present study, the damping capacity decreased with the increasing frequencies almost in the whole measuring temperature ranges when testing frequencies below 20 Hz (Fig. 4). Thus, thermoelastic damping has no contribution to improving the damping capacity of these composites in the frequency range, because the Zener relaxation frequency of the Al matrix composites is about 160 Hz.

Thermoelastic damping is caused by the energy dissipated by the irreversible heat flow generated by stress-induced thermal gradients. The thermoelastic damping is more prominent when the material undergoes a heterogeneous deformation [28]. The kind of heterogeneous deformation exists in the DMA specimens of the coated composites. In this present study, the measured damping capacity of the coated composites increased with the increasing frequencies in the frequency range of 40–70 Hz (Fig. 6), suggesting that the thermoelastic damping is the dominant damping mechanism in this frequency range.

In order to know more information on the frequency dependency of the damping capacity for the coated composites in the entire frequency range used here, a comparison of the damping capacity for the 10ABOw/SnBiO/Al composite at 0.5 and 70 Hz is represented in Fig. 9. A point of intersection at about 113 °C appeared in Fig. 9. When the temperature is below 113 °C, the damping values of the coated composite are higher at higher frequencies. When the temperature exceeds 113 °C, the damping values of the coated composite are higher at lower frequencies. It is indicated that the damping mechanisms had changed below and above the critical temperature (point of intersection).

A critical temperature also exists in the damping-temperature curves of the 20ABOw/SnBiO/Al and the 6ABOw/SnBiO/Al composites at 0.5 and 70 Hz, respectively. The temperatures of the point of intersection in the 20ABOw/SnBiO/Al and 6ABOw/SnBiO/Al were to be 129 °C and 108 °C, respectively.

According to the Granato-Lüecke (GL) dislocation model as strain amplitude increases to the critical strain amplitude, the dislocation may break away in a snowslide-like mode from the weak pinning and the dislocation damping increases quickly. Thus, at higher strain amplitudes, the dislocation damping mechanism becomes dominant. If the strain amplitude was fixed, as a result, the coated composites exhibited higher damping capacities at higher frequencies then when the temperature was below the critical temperature.

The presence of the low-melting-point phase at the interface led to the interface slip (whisker/interlayer) easily owing to the Bi–Sn eutectic softening during the temperature rising. Therefore, the damping capacity of the coated composites increased with the increasing temperature. The higher the temperature is, the more the contribution of the interface damping (whole interface). The contribution of the dislocation damping decreases with the increasing temperature. The point of intersection may become a breaking point for dominant damping mechanisms of the coated composites. When the temperature is below the critical temperature point, the damping mechanism of the coated composites is attributed to the dislocation damping; when the temperature is above the critical temperature point, the interface damping becomes the main damping mechanism for the coated composites.

It is significant to note that the critical temperature is below the temperature of the damping peak, which gives further proof that the damping mechanism of the peak in the present study is to relate to the interfacial slip at the whisker/interlayer and the interlayer/Al interfaces. Furthermore, it is worth noting that the critical temperature decreased with the increasing of the coating contents, indicating that the energy dissipation caused by the interface slip will occur easily when the coating contents are high.

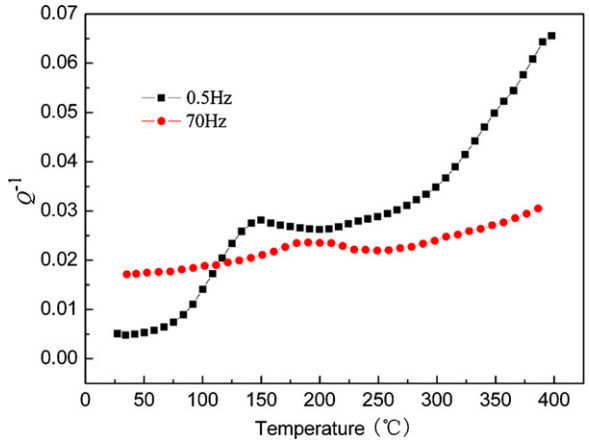

Fig. 9. Damping capacity of the 10ABOw/SnBiO/Al composite at different frequencies.

5. Conclusions

1. The mixed coatings play a very important role in the damping properties of the coated composites. The damping capacities of the coated composites strongly depend on not only the coating contents but also the strain amplitude (for lower frequencies).
2. One pronounced damping peak can be observed in the coated composites, the activation energies of the damping peak in the 10ABOw/SnBiO/Al composite is calculated to be 1.23 and the damping mechanism is mainly attributed to the interfacial sliding of the molten Bi–Sn eutectic.
3. The measurement frequency strongly affects the damping capacities of the coated composites. The damping capacities decrease and the damping peak shifts towards higher temperatures with the increasing frequency (below 20 Hz), exhibiting the characteristics of a relaxation type. However, the damping value increases with the increasing frequency (above 40 Hz), where thermoelastic damping becomes the dominant damping mechanism.
4. A critical temperature in the damping-temperature curves of the coated composites has been found for the first time when the vibration frequencies changed. The dominant damping mechanisms changed from the dislocation damping to the interfacial damping below and above the critical temperature, respectively. The critical temperature decreases with the increasing of coating contents.

References

[1] J.H. Gu, X.N. Zhang, M.Y. Gu, J. Alloys Compd. 381 (2004) 182–187.
[2] R. Schaller, J. Alloys Compd. 355 (2003) 131–135.
[3] C. Wang, Z. Zhu, Scripta Mater. 38 (1998) 1739–1743.
[4] X.Q. Zhang, H.W. Wang, L.H. Liao, N.H. Ma, Compos. Sci. Technol. 67 (2007) 720–727.
[5] K.S. Foo, W.M. Banks, A.J. Craven, Composite 25 (7) (1994) 677–683.
[6] T.P.D. Rajan, R.M. Pillai, B.C. Pai, J. Mater. Sci. 33 (14) (1998) 3491–3503.
[7] L. Parrina, R. Schaller, Acta Mater. 44 (1996) 4881–4888.
[8] E. Carreno-morelli, S.E. Urreta, R. Schaller, Acta Mater. 48 (2000) 4725–4733.
[9] J.H. Gu, X.N. Zhang, M.Y. Gu, Mater. Lett. 59 (2005) 180–184.
[10] J.H. Gu, X.N. Zhang, Y.F. Qiu, M.Y. Gu, Compos. Sci. Technol. 65 (2005) 1736–1742.
[11] L. Shen, J.J. Li, Int. J. Solids Struct. 40 (2003) 1393–1409.
[12] E.M. Ruiz-Navas, M.L. Delgado, J.M. Torralba, J. Mater. Sci. 41 (12) (2006) 3735–3741.
[13] E.M. Ruiz-Navas, M.L. Delgado, B. Torralba, Composites Part A 40 (8) (2009) 1283–1290.
[14] X.N. Zhang, Ph.D. Dissertation, Shanghai Jiao Tong University, Shanghai China, 1997, p. 81.
[15] H.Y. Yue, W.D. Fei, Z.J. Li, L.D. Wang, Mater. Sci. Eng. 441 (1–2) (2006) 197–201.
[16] J. Hu, W.D. Fei, C. Li, C.K. Yao, J. Mater. Sci. Lett. 13 (24) (1994) 1797–1799.
[17] J. Hu, X.F. Wang, S.W. Tang, Compos. Sci. Technol. 68 (2008) 2297–2299.
[18] G. Liu, W.C. Ren, Y.L. Sun, J. Hu, Mater. Sci. Eng. 527A (2010) 5136–5143.
[19] G. Liu, J. Hu, Mater. Sci. Eng., 2011, in press.
[20] A.S. Nowick, B.S. Berry, Anelastic Relaxation in Crystalline Solids, Academic Press, New York, 1972.
[21] C.S. Changqi, Z. Pinglin, Binary Alloy Phase-Diagrams, Originally published in Japanese by AGNE Gijutsu Center, Co., Ltd., Tokyo, Japan, 1992.
[22] J. Hu, R.S. Luo, W.D. Fei, C.K. Yao, J. Mater. Sci. Lett. 18 (1999) 1525–1527.
[23] R.J. Arsenault, N. Shi, Mater. Sci. Eng. 81 (1986) 175–187.
[24] G.H. Fan, L. Geng, Z.Z. Zheng, G.S. Wang, Scripta Mater. 59 (2008) 534–537.
[25] J. Hu, X.F. Wang, Z.Z. Zheng, J. Appl. Phys. 107 (2010) 023513.
[26] C. Zener, Elasticity and Anelasticity of Metals, The University of Chicago, Chicago (IL), 1948.
[27] H.X. Zhang, M.Y. Gu, J. Alloys Compd. 426 (2006) 247–252.
[28] R. Bauri, M.K. Surappa, Metall. Mater. Trans. A 36 (3) (2005) 667–673.